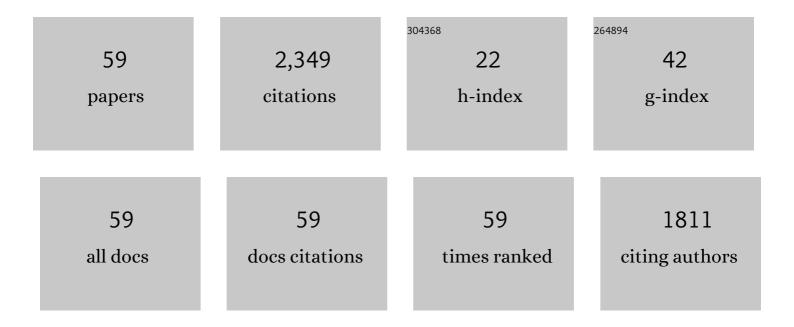
Tadamichi Akagi

List of Publications by Year in descending order

Source: https://exaly.com/author-pdf/7880658/publications.pdf Version: 2024-02-01



#	Article	lF	CITATIONS
1	Microvascular Density in Glaucomatous Eyes With Hemifield Visual Field Defects: An Optical Coherence Tomography Angiography Study. American Journal of Ophthalmology, 2016, 168, 237-249.	1.7	204
2	Peripapillary and Macular Vessel Density in Patients with Glaucoma and Single-Hemifield Visual Field Defect. Ophthalmology, 2017, 124, 709-719.	2.5	202
3	Progressive Macula Vessel Density Loss in Primary Open-Angle Glaucoma: A Longitudinal Study. American Journal of Ophthalmology, 2017, 182, 107-117.	1.7	165
4	Reproducibility of Optical Coherence Tomography Angiography Macular and Optic Nerve Head Vascular Density in Glaucoma and Healthy Eyes. Journal of Glaucoma, 2017, 26, 851-859.	0.8	106
5	Optical Coherence Tomography Angiography Macular Vascular Density Measurements and the Central 10-2 Visual Field in Glaucoma. Journal of Glaucoma, 2018, 27, 481-489.	0.8	98
6	Retinal Nerve Fiber Layer Defects in Highly Myopic Eyes with Early Glaucoma. , 2012, 53, 6472.		90
7	Three-Dimensional Imaging of Lamina Cribrosa Defects in Glaucoma Using Swept-Source Optical Coherence Tomography. , 2013, 54, 4798.		89
8	Macula Vessel Density and Thickness in Early Primary Open-Angle Glaucoma. American Journal of Ophthalmology, 2019, 199, 120-132.	1.7	87
9	Conjunctival and Intrascleral Vasculatures Assessed Using Anterior Segment Optical Coherence Tomography Angiography in Normal Eyes. American Journal of Ophthalmology, 2018, 196, 1-9.	1.7	79
10	Cause and prognosis of neurologically isolated third, fourth, or sixth cranial nerve dysfunction in cases of oculomotor palsy. Japanese Journal of Ophthalmology, 2008, 52, 32-35.	0.9	75
11	Recent advances in OCT imaging of the lamina cribrosa. British Journal of Ophthalmology, 2014, 98, ii34-ii39.	2.1	69
12	Microstructure of Peripapillary Atrophy and Subsequent Visual Field Progression in Treated Primary Open-Angle Glaucoma. Ophthalmology, 2016, 123, 542-551.	2.5	61
13	In Vivo Imaging of Lamina Cribrosa Pores by Adaptive Optics Scanning Laser Ophthalmoscopy. , 2012, 53, 4111.		58
14	Otx2Homeobox Gene Induces Photoreceptor-Specific Phenotypes in Cells Derived from Adult Iris and Ciliary Tissue. , 2004, 45, 4570.		57
15	Peripapillary Scleral Deformation and Retinal Nerve Fiber Damage in High Myopia Assessed With Swept-Source Optical Coherence Tomography. American Journal of Ophthalmology, 2013, 155, 927-936.e1.	1.7	55
16	Lamina Cribrosa Defects and Optic Disc Morphology in Primary Open Angle Glaucoma with High Myopia. PLoS ONE, 2014, 9, e115313.	1.1	53
17	Asymmetry Analysis of Macular Inner Retinal Layers for Glaucoma Diagnosis. American Journal of Ophthalmology, 2014, 158, 1318-1329.e3.	1.7	53
18	Different characteristics of rat retinal progenitor cells from different culture periods. Neuroscience Letters, 2003, 341, 213-216.	1.0	45

Ταδαμιςμι Ακάςι

#	Article	IF	CITATIONS
19	Alterations in the Neural and Connective Tissue Components of Glaucomatous Cupping After Glaucoma Surgery Using Swept-Source Optical Coherence Tomography. , 2014, 55, 477.		45
20	The Association Between Macula and ONH Optical Coherence Tomography Angiography (OCT-A) Vessel Densities in Glaucoma, Glaucoma Suspect, and Healthy Eyes. Journal of Glaucoma, 2018, 27, 227-232.	0.8	42
21	Iris-Derived Cells from Adult Rodents and Primates Adopt Photoreceptor-Specific Phenotypes. , 2005, 46, 3411.		41
22	Microcystic Inner Nuclear Layer Changes and Retinal Nerve Fiber Layer Defects in Eyes with Glaucoma. PLoS ONE, 2015, 10, e0130175.	1.1	38
23	Wide 3-Dimensional Macular Ganglion Cell Complex Imaging with Spectral-Domain Optical Coherence Tomography in Glaucoma. , 2012, 53, 4805.		37
24	Sensitivity and specificity for detecting early glaucoma in eyes with high myopia from normative database of macular ganglion cell complex thickness obtained from normal non-myopic or highly myopic Asian eyes. Graefe's Archive for Clinical and Experimental Ophthalmology, 2015, 253, 1143-1152.	1.0	36
25	Rates of Local Retinal Nerve Fiber Layer Thinning before and after Disc Hemorrhage in Glaucoma. Ophthalmology, 2017, 124, 1403-1411.	2.5	36
26	Frequency-doubling technology and retinal measurements with spectral-domain optical coherence tomography in preperimetric glaucoma. Graefe's Archive for Clinical and Experimental Ophthalmology, 2013, 251, 129-137.	1.0	32
27	Progression of Primary Open-Angle Glaucoma in Diabetic and Nondiabetic Patients. American Journal of Ophthalmology, 2018, 189, 1-9.	1.7	30
28	Deep-Layer Microvasculature Dropout by Optical Coherence Tomography Angiography and Microstructure of Parapapillary Atrophy. , 2018, 59, 1996.		29
29	Biometric Features of Peripapillary Atrophy Beta in Eyes with High Myopia. , 2011, 52, 6706.		28
30	Transient Ciliochoroidal Detachment After Ab Interno Trabeculotomy for Open-Angle Glaucoma. JAMA Ophthalmology, 2016, 134, 304.	1.4	27
31	Optic disc microvasculature dropout in primary open-angle glaucoma measured with optical coherence tomography angiography. PLoS ONE, 2018, 13, e0201729.	1.1	26
32	Comparative outcomes of trabeculotomy ab externo versus trabecular ablation ab interno for open angle glaucoma. Japanese Journal of Ophthalmology, 2018, 62, 201-208.	0.9	20
33	Comparison of Longitudinal Changes in Functional and Structural Measures for Evaluating Progression of Glaucomatous Optic Neuropathy. , 2015, 56, 5477.		18
34	Visualization of the Lamina Cribrosa Microvasculature in Normal and Glaucomatous Eyes: A Swept-source Optical Coherence Tomography Angiography Study. Journal of Glaucoma, 2018, 27, 1032-1035.	0.8	17
35	Retinal Blood Flow Velocity Change in Parafoveal Capillary after Topical Tafluprost Treatment in Eyes with Primary Open-angle Glaucoma. Scientific Reports, 2017, 7, 5019.	1.6	16
36	Anterior Segment Optical Coherence Tomography Angiography Imaging of Conjunctiva and Intrasclera in Treated Primary Open-Angle Glaucoma. American Journal of Ophthalmology, 2019, 208, 313-322.	1.7	16

Ταδαμιςμι Ακάςι

#	Article	IF	CITATIONS
37	Longitudinal change in choroidal thickness after trabeculectomy in primary open-angle glaucoma patients. Japanese Journal of Ophthalmology, 2017, 61, 105-112.	0.9	15
38	A case of cyclosporine-induced optic neuropathy with a normal therapeutic level of cyclosporine. Japanese Journal of Ophthalmology, 2010, 54, 102-104.	0.9	13
39	Association of Bruch's membrane opening and optic disc morphology to axial length and visual field defects in eyes with primary open-angle glaucoma. Graefe's Archive for Clinical and Experimental Ophthalmology, 2018, 256, 599-610.	1.0	12
40	Pilot study assessing the structural changes in posttrabecular aqueous humor outflow pathway after trabecular meshwork surgery using swept-source optical coherence tomography. PLoS ONE, 2018, 13, e0199739.	1.1	12
41	Longitudinal changes in superficial microvasculature in glaucomatous retinal nerve fiber layer defects after disc hemorrhage. Scientific Reports, 2020, 10, 22058.	1.6	12
42	Structural dissociation of optic disc margin components with optic disc tilting: a spectral domain optical coherence tomography study. Graefe's Archive for Clinical and Experimental Ophthalmology, 2016, 254, 343-349.	1.0	11
43	Evaluation of Structure-Function Relationships in Longitudinal Changes of Glaucoma using the Spectralis OCT Follow-Up Mode. Scientific Reports, 2018, 8, 17158.	1.6	10
44	Prediction of trabecular meshwork-targeted micro-invasive glaucoma surgery outcomes using anterior segment OCT angiography. Scientific Reports, 2021, 11, 17850.	1.6	10
45	Clustering of Combined 24-2 and 10-2 Visual Field Grids and Their Relationship With Circumpapillary Retinal Nerve Fiber Layer Thickness. , 2016, 57, 3203.		9
46	Short-Term Effects of Different Types of Anti-Glaucoma Eyedrop on the Sclero-Conjunctival Vasculature Assessed Using Anterior Segment OCTA in Normal Human Eyes: A Pilot Study. Journal of Clinical Medicine, 2020, 9, 4016.	1.0	9
47	Lacrimal Canaliculus Imaging Using Optical Coherence Tomography Dacryography. Scientific Reports, 2018, 8, 9808.	1.6	8
48	Morphological changes after trabeculectomy in highly myopic eyes with high intraocular pressure by using swept-source optical coherence tomography. American Journal of Ophthalmology Case Reports, 2016, 3, 54-60.	0.4	7
49	Baerveldt or Ahmed glaucoma valve implantation with pars plana tube insertion in Japanese eyes with neovascular glaucoma: 1-year outcomes. Clinical Ophthalmology, 2018, Volume 12, 2439-2449.	0.9	7
50	Association between Rates of Retinal Nerve Fiber Layer Thinning and Previous Disc Hemorrhage in Glaucoma. Ophthalmology Glaucoma, 2018, 1, 23-31.	0.9	7
51	Glaucoma Tube Changes After Suture Lysis Assessed by High-Resolution Anterior Segment Optical Coherence Tomography. JAMA Ophthalmology, 2016, 134, e153674.	1.4	5
52	Association between topical β-blocker use and asthma attacks in glaucoma patients with asthma: a cohort study using a claims database. Graefe's Archive for Clinical and Experimental Ophthalmology, 2022, 260, 271-280.	1.0	5
53	Association between the CDKN2B-AS1 Gene and Primary Open Angle Glaucoma with High Myopia in Japanese Patients. Ophthalmic Genetics, 2016, 37, 242-244.	0.5	4
54	Association between Rates of Retinal Nerve Fiber Layer Thinning after Intraocular Pressure–Lowering Procedures and Disc Hemorrhage. Ophthalmology Glaucoma, 2020, 3, 7-13.	0.9	4

#	Article	IF	CITATIONS
55	Relationship between Intraocular Pressure and Coffee Consumption in a Japanese Population without Glaucoma. Ophthalmology Glaucoma, 2021, 4, 268-276.	0.9	4
56	Photoreceptors Derived from Adult Iris Tissue: Prospects for Retinal Transplantation. Seminars in Ophthalmology, 2005, 20, 11-15.	0.8	3
57	Longitudinal changes in complete avascular area assessed using anterior segmental optical coherence tomography angiography in filtering trabeculectomy bleb. Scientific Reports, 2021, 11, 23418.	1.6	2
58	Reply. American Journal of Ophthalmology, 2016, 170, 248-249.	1.7	0
59	Reply. Ophthalmology, 2018, 125, e22-e23.	2.5	0